International Journal of Computational Intelligence Systems and Applications. Volume 11, Issue 1, (2024) 9-17
http://www.cayley-nielson.com/ijcisa/

YOLO-SOD-DLK: A YOLOv8-based Network for Astrocytes Detection in Immunofluorescence Photographs

Zhixin Li[1], Xiaoqian Huo[1]
[1] North China University of Science and Technology, Tangshan, Hebei, China
E-mail: *1034990898@qq.com*

Abstract

Astrocytes perform important homeostatic functions in the central nervous system. It's one of the important means to capture photographs of dual-labeled immunofluorescence staining slices by confocal laser scanning microscopy to research the expression of inflammatory factors in astrocytes. This paper introduced a YOLOv8-based network named YOLO-SOD-DLK to quantify positive expression of inflammatory factors in astrocytes. The D-LKA modules were integrated into YOLOv8 framework to improve the performance of recognizing dense small objects and irregular objects in immunofluorescence staining photographs. The dataset consists of 2083 dual-labeled immunofluorescence staining photographs from multiple basic medical experiments related to the expression of inflammatory factors in astrocytes. Our model reached 92.65% in the most important evaluation matrix, mAP@50. The results demonstrated that our proposed models can quantify accurately the degree of positive expression of inflammatory factors in astrocytes and avoid effectively artificial error.

Keywords: Astrocyte, Immunofluorescence, YOLO, D-LKA.

1. Introduction

Astrocytes play an important dual role in the complex regulation of local immune reaction and maintaining the function of neurons, as well as undergo inflammatory transformation during infection, acute injury and neurodegenerative diseases [1,2]. The immunofluorescence staining photographs of rat brain tissue are usually used to in research of the positive expression of inflammatory factors in astrocytes. Due to the complex background, large number of cells and high similarity between categories in immunofluorescence staining photographs, the workload of manual statistics is too heavy and the accuracy and reliability of results are usually affected by inconsistent standards, high complexity of images and heavy workload.

With the rapid development of image segmentation and object detection techniques based on deep learning, it has become a more efficient and reliable way to analyze immunofluorescence staining photographs and count automatically by artificial intelligence technology. In this paper, we propose YOLO-SOD-DLK network to detect astrocytes with positive expression of TNF-α and IL-1b inflammatory factors, as well as all astrocyte nuclei in the immunofluorescence staining photographs.

The models of YOLO series can effectively detect the objects with different scales by multi-level feature fusion strategy, and have strong robustness and generalization ability which leads to applicability for various scenarios. Multiple improvements are made in YOLOv8 on the base of previous versions including the introduction of architectures of CSPDarknet53, PANet and so on. CSPDarknet53 backbone network significantly enhances the ability of model to perceive spatial information and the efficiency of

object detection due to better feature representation。PANet (Path Aggregation Network) in neck of YOLOv8 enhances the capability of detecting targets with different sizes by aggregating feature maps at different scales.

This paper proposes the YOLO-SOD-DLKA network by introducing the D-LKA (Deformable Large Kernel Attention) attention module into the YOLOv8 framework to detect dense irregular small targets in immunofluorescence staining photographs. D-LKA module combines the large convolution kernel with the deformable convolution to recognize various forms of organizations flexibly and accurately, reduce the overfitting and improve the generalization ability, which can significantly enhance the capability of comprehension of complex details and global information of immunofluorescence staining photographs.

2. Related work

In 2015, Ross Girshick and Jeff Donahue designed R-CNN framework for object detection with providing region proposals by selective search algorithm, extracting feature map from region proposals by CNN and SVM for classification [3]. Shaoqing Ren, Kaiming He et al. proposed Faster R-CNN network which unified RPN and Fast R-CNN network and significantly improved detection efficiency by sharing single CNN by all regions [4]. Joseph Redmon and Santosh Divvala reframed object detection as a single regression problem and designed YOLO (You Only Look Once) network which used a single convolutional neural network to predict bounding boxes and class probabilities directly from full images in one evaluation [5]. From YOLOv2 to YOLOv5，Anchor box，FPN, CBN, PAN, SAM，SPPF, Mosaic data augmentation etc. were introduced to improve performance gradually and construct the network consisting of backbone, neck and head [6, 7, 8].

Zhou Hao and Fei Peng solved the problem of deep scattering of large organizational samples by combining deep learning with optical microscopy to improve imaging spatial resolution, with single-molecule localization microscopy to improve imaging temporal resolution [9]. Reza Azad, Leon Niggemeier et al. present Deformable Large Kernel Attention module to improve the ability of detecting small and irregular objects especially in complex background by combining the large convolution kernel with the deformable convolution [10].

3. Method

Three photographs are taken by a confocal laser scanning microscope for each frozen hippocampal section after immunofluorescence staining. The green fluorescent areas in the first photograph are astrocytes stained with GFAP markers, the red fluorescent areas in the second photograph are the expression of inflammatory factors in the cytoplasm, and the blue areas in the third photograph are the stained nucleus. The three photographs of the same section are overlapped to form the immunofluorescence staining photograph, as shown in Fig. 1. The yellow areas represent astrocytes with positive expression of inflammatory factors, the small blue circular areas represent the nucleus of astrocytes, and the areas of dense blue circles are granular layers, which are three types of objects to be detected.

In this paper, we designed an object detection network based on deep learning to detect astrocyte nucleus (AN) and astrocytes with positive expression of inflammatory factors (AP), and the ratio of their quantities as the quantitative indicator (QIoAP) of inflammatory response of central nervous system.

$$QIoAP = \frac{AP}{AN+AP} \tag{1}$$

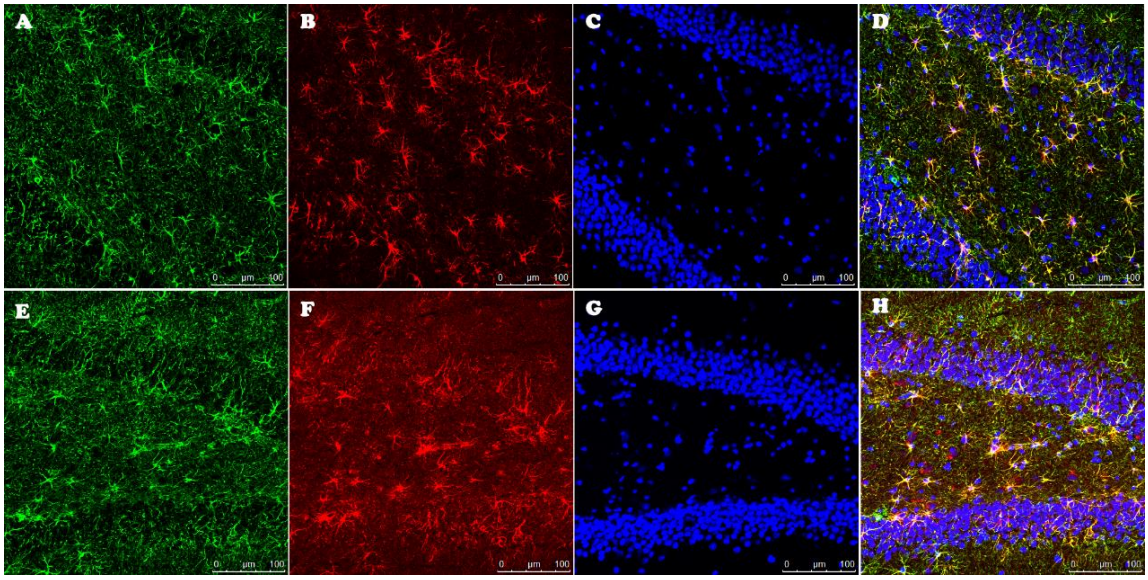

Fig.1. Immunofluorescence staining photograph of astrocytes. (A) ,(E) astrocytes stained with GFAP markers; (B),(F) the expression of inflammatory factors in the cytoplasm; (C),(G) the stained nucleus; (D),(H) overlaid photographs.

The object detection technology based on deep learning has been widely applied in the biomedical field. Lourdes et al. detected diabetes retinopathy in retinal images by Faster R-CNN model [11]. Zheng and Sun Yi et al. used CNN-based approach to detect pulmonary nodules in CT images [12]. As the most successful object detection frame-work in recent years, YOLO has made remarkable achievement in rapid detection and localization of diseases and abnormal areas in medical images, such as lung nodules, heart disease, and fundus lesions. Xue Linyan and Li Xuanang et al. proposed a realtime multiclass detection model for colonoscopic polyps based on modified YOLOv5s [13]. Joseph Sobek et al. reported a 3-D object detection framework MedYOLO which achieved high performance on large-sized structure in medical images [14].

We built YOLO-SOD-DLKA network on YOLOv8 as base framework to detect astrocytes and nucleus. YOLOV8 architecture is composed of Backbone, Neck and Head structures. Backbone structure is responsible for feature extraction with a series of convolution layers and improves performance by ResNet and Bottleneck modules. Compared to previous versions, C2f module, depthwise separated convolution and dilated convolution in Backbone of YOLOv8 enhance capability of feature extraction. Neck structure consists of PPF, PAA, and PAN modules which is responsible for multiscale feature fusion to enhance feature expression capability. Head structure is re-sponsible for object detection and classification, where the detection head is responsible for bounding box regression and object confidence, and the classification head is responsible for outputting the probability of each category. In addition, YOLOv8 uses DFL Loss+IOU Loss as the classification loss and Task Signed Assign as the sample matching method.

Due to the presence of numerous small targets with irregular shapes and colors in the immunofluorescence staining photographs of astrocytes, especially the subtle differences between infected and uninfected astrocytes, as well as between the nuclei of astrocytes and microglia, we made the following improvements on base framework. Firstly, YOLOv8 designed three detection heads, corresponding to feature map sizes of 80×80, 40×40, and 20×20, to respectively detect targets of small, medium, and large scales. It's lack of the ability to detect objects with smaller size such as astrocyte nuclei because the feature maps of low layer created by Backbone and Neck were ignored. We built a feature map of size 160×160

by additional upsampling and concatenation in Neck structure and added a smaller detection head to improve the accuracy of small targets detection

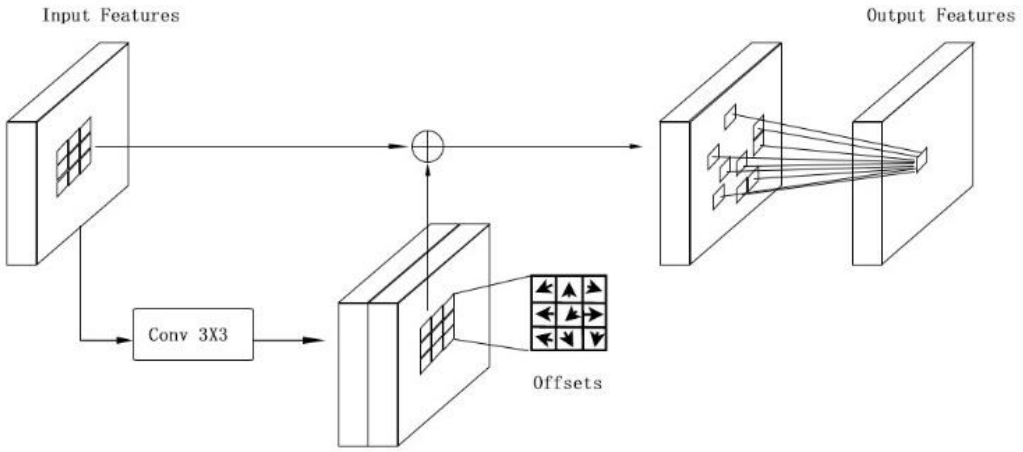

Fig. 2. Architecture of Deform Depth-wise Conv2D Block

Secondly, we embedded D-LKA module into YOLOv8 network to effectively fuse features at different levels to improve the ability of perceiving small and irregular shapes. D-LKA (Deformable Large Kernel Attention) integrates large convolutional kernel and deformable convolutional to achieve flexible network architecture that can effectively detect objects with irregular shape and size, as well as avoid high computational cost. As shown in Fig. 2, Deform Depth-wise Conv2D module generates an offset table of position through a single convolution operation and then applies the offsets to the corresponding positions in the next convolution operation to implement deformable convolution.

In Deformable LKA module, an input feature map X1 $\in$ RC×H×W goes through a Conv2D and GELU operation and the result is a feature map X2. X2 goes through two Deform Depth-wise Conv2D modules and a Conv2D, and the result is X3. Then X2 multiplies X3, goes through the last Conv2D, adds X1 to generate output feature map YC×H×W. The computational formula for the Deformable LKA module is as follows and the architecture is shown in Fig. 3.

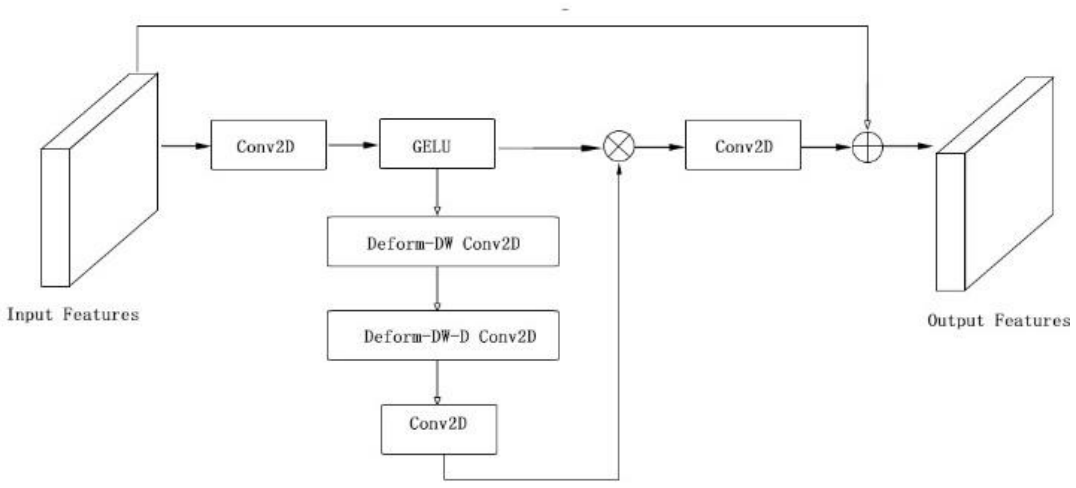

Fig. 3. Architecture of Deform Depth-wise Conv2D Block.

$$X2 = GELU(Conv2D(X1)) \quad (2)$$

$$X3 = Conv2D(Deform\text{-}DW\ Conv2D(X2)) \quad (3)$$

$$X4 = Conv2D\ (Deform\text{-}DW\text{-}D(X3)) \quad (4)$$

$$Y = X1 \oplus Conv2D\ (X2 \otimes X4) \quad (5)$$

We designed C2f-DLK module to replaced the C2f modules in YOLOv8, as shown in Fig. 4, in which the output of Bottlenecks in C2f module was sent to D-LKA module and the result was concatenated with the input feature map, and then the last convolution generated the output feature map.

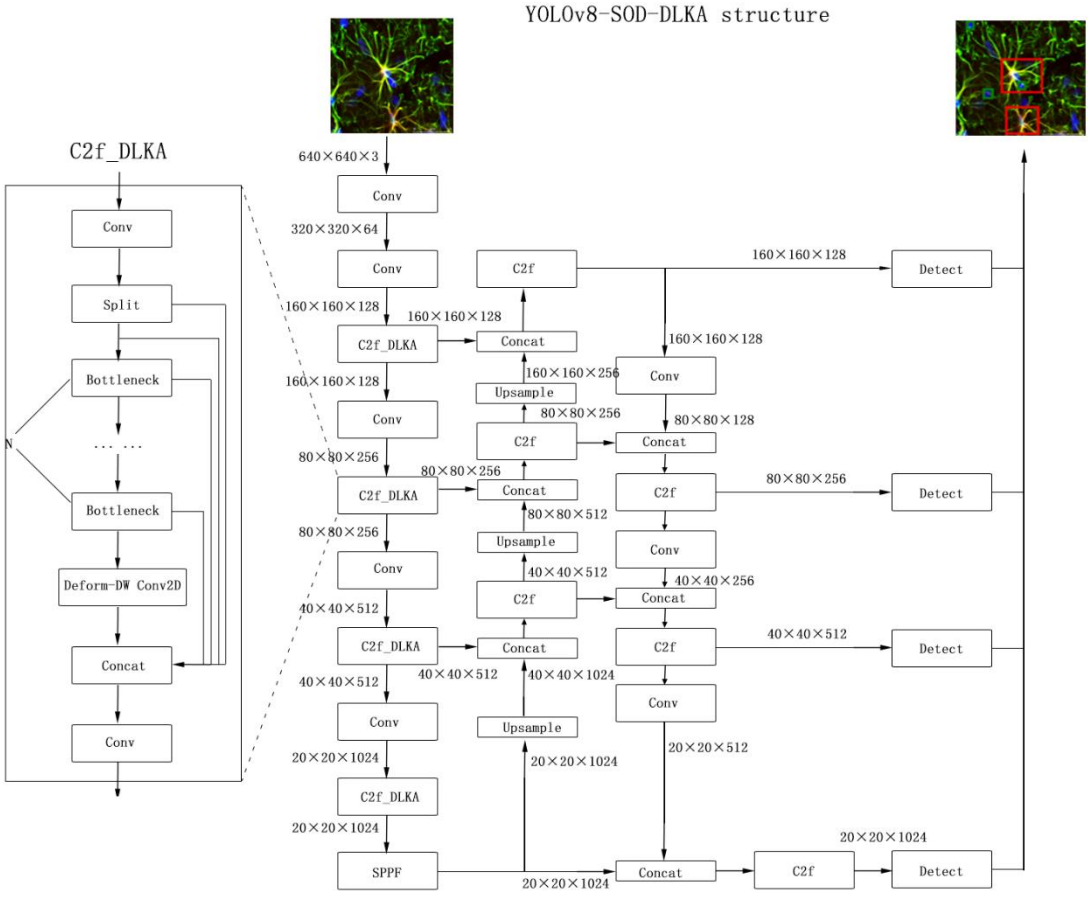

Fig. 4. Architecture of YOLO-SOD-DLKA

4. Experiments

We collected 2083 immunofluorescence photographs of astrocytes (scale 1:100000) from various experiments from 2015 to 2020, including 1971 successfully stained fluorescence photos and 112 failed ones. 54716 astrocyte nuclei and 20674 astrocytes with positive expression of inflammatory factors were labeled with Labelme tool. As shown Figure 5, the nuclei and astrocytes were labeled with rectangles for object detection.

Three evaluation metrics were used to evaluated YOLO-SOD-DLK, precision, re-call and mAP. Precision is the proportion of true positive samples among the samples predicted by the model as positive samples, defined as follows

$$Precision = \frac{TP}{TP+FP} \quad (6)$$

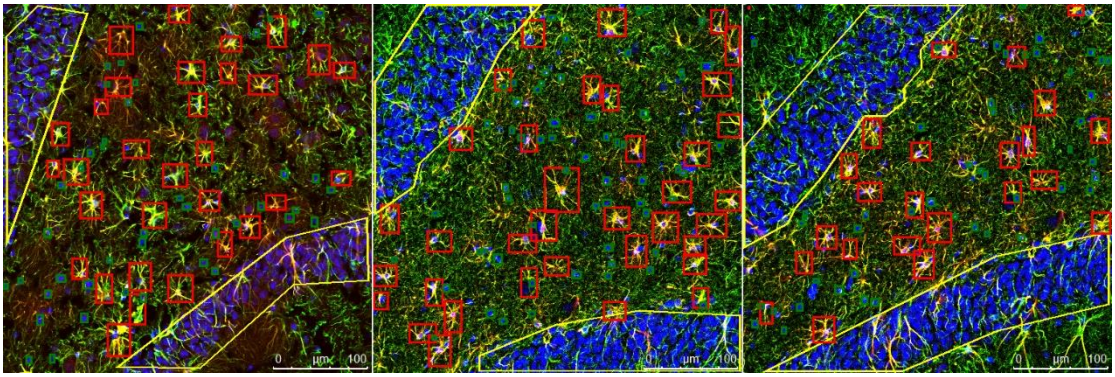

Fig. 5. labels in immunofluorescence photographs of astrocytes (scale 1:100000)

TP (True Positive) denotes the number of instances predicted correctly as positive; FP (False Positive) denotes the number of instances predicted incorrectly as positive.

Recall measures the ratio of correctly predicted positive samples to all positive samples. The higher the recall rate, the more accurately the model can detect positive samples.

$$Recall = \frac{TP}{TP+FN} \tag{7}$$

FN (False Negative) denotes the number of instances predicted incorrectly as negative.

AP (Average Precision) is precision averaged across all values of recall between 0 and 1. We created precision-recall curve with recall as horizontal axis and precision as vertical axis and the area enclosed by the PR curve and the coordinate axis is AP, computed as follows

$$AP = \int_0^1 Precision(Recall) d(Recall) \tag{8}$$

The average AP of all categories is mAP that indicates the detection performance on the entire dataset of model. mAP@50 is mAp on condition of IoU threshold of 0.5 and mAP@50:95 is the average mAPs that are computed on IoU threshold from 0.5 to 0.95 with interval 0.05.

4. Result

We added a feature map of low layer with the size of 160×160 in Neck structure of YOLOv8 and an additional detecting head for it to detect small size objects and named it YOLO-SOD model. Then D-LK model was integrated into Backbone structure of YOLO-SOD in order to improve the performance of detecting objects with irregular shape under complex background, which is named YOLO-SOD-DLK model. We trained YOLOv8 and the two new models on 2083 immunofluorescence photograph, train set with size of 1800, validation set with size of 200 and test set with size of 83, with learning rate of 0.01, batch size of 8 and epoch of 200.

As shown in Fig. 6, YOLO-SOD-DLKA model outer-performs YOLOv8 on overlapping small and irregular objects. The details of comparison are shown in Fig. 7.

As shown in Table 2， YOLO-SOD achieved improvement of 0.08% and 0.09% over YOLOv8 on precision and recall, 0.13% on AP@0.5, which proved that smaller detection head for low layer feature map(160×160) was benefit to detect astrocyte nucleus. YOLO-SOD-DLKA improved the recall, AP@0.5 and AP@0.5:0.95 by 0.04%，0.01% and 0.02% compared to YOLO-SOD, due to the ability of D-LKA module to detect objects under complex background. See Table 1 for details.

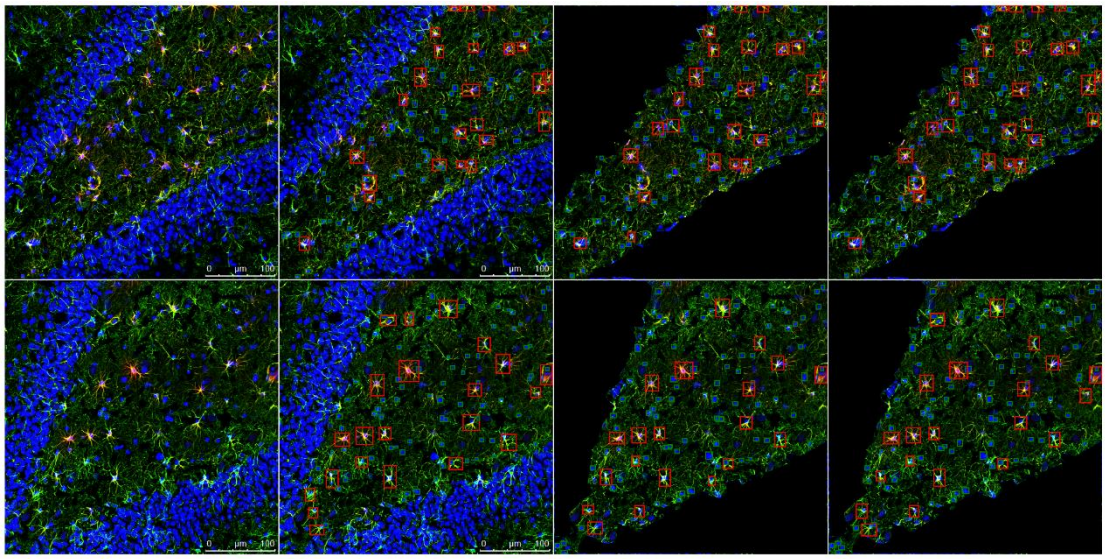

(a) (b) (c) (d)

Fig. 6 Qualitative comparison of the results from YOLOv8 and YOLO-SOD-DLKA: (a) original image (b) ground truth (c) YOLOv8 result (d) YOLO-SOD-DLKA result

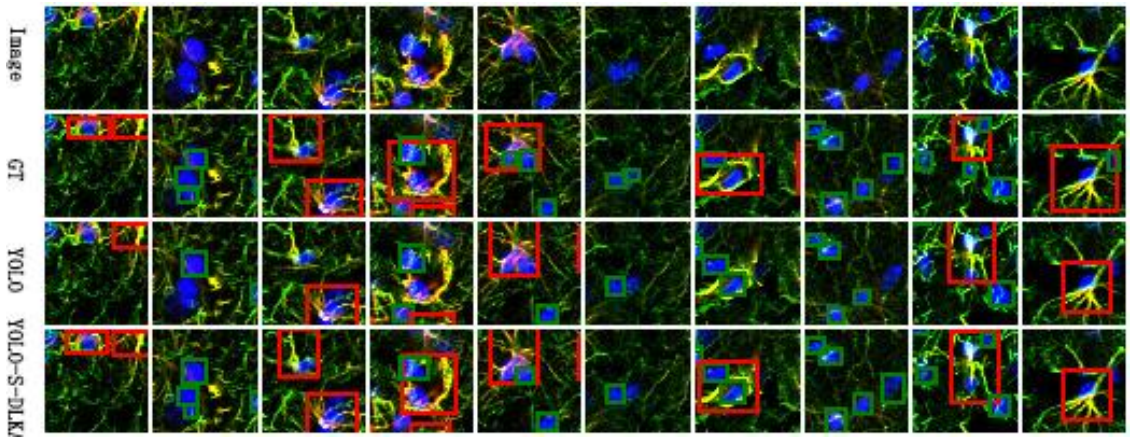

Fig. 7. Details of comparison between the results from YOLOv8 and YOLO-SOD-DLKA

Table 1. Result of astrocyte nucleus detection

Model	Precision(%)	Recall(%)	AP@0.5(%)	AP@0.5:0.95（%）
YOLOv8x	90.35	83.47	90.95	77.95
YOLO-SOD	90.43	83.58	91.08	78.01
YOLO-SOD-DLKA	90.42	83.62	91.09	78.03

Table 2 shows that YOLO-SOD-DLKA achieved the best performance on all four evaluation metrics, which proved that D-LKA module had strong ability in detecting irregular objects such as astrocytes.

Table 3 shows the comprehensive object detection result of all classes. YOLO-SOD-DLKA achieved 91.86% on mAP@0.5 which is 0.25% higher than the YOLOv8 and 0.19% than YOLO-SOD, and 76.63% on mAP@0.5:0.95 which is 0.47% higher than YOLOv8 and 0.42% than YOLO-SOD. Our proposed architecture improved the precision of astrocytes and nucleus detection and classification based on YOLOv8 framework and was able to provide accurate and reliable data to quantify the degree of positive

expression of inflammatory factor in astrocytes.

Table 2. Result of astrocytes with positive expression of inflammatory factors detection

Model	Precision(%)	Recall(%)	AP@0.5(%)	AP@0.5:0.95(%)
YOLOv8x	92.25	86.18	92.27	80.36
YOLO-SOD	92.22	86.20	92.26	80.41
YOLO-SOD-DLKA	92.41	86.33	92.62	81.23

Table 3. Comparation of overall results from YOLOv8, YOLO-SOD and YOLO-SOD-DLKA

Model	Precision(%)	Recall(%)	mAP@0.5(%)	mAP@0.5:0.95(%)
YOLOv8x	90.92	84.29	91.61	79.16
YOLO-SOD	90.96	84.38	91.67	79.21
YOLO-SOD-DLKA	91.03	84.43	91.86	79.63

5. Discussion

The immunofluorescence photography is a common technology in animal brain cell immunity experiments which rely on accurate classification and analysis of the number, morphology, and status of various cells and organelles in the photographs. The manual counting and classification not only require a large amount of work, but also leads to deviations in experimental data on account of the characteristics of immunofluorescence photograph such as complex background, small and dense objects, irregular shape and blurred boundaries between of cells and organelles.

With the rapid development of image segmentation and object detection technologies based on deep learning and computer vision, it's reasonable and applicative to improve the accuracy and efficiency of immunofluorescence photographs analysis by AI technologies. The representative frameworks of image segmentation and object detection include the U-Net series, YOLO series and the Transformer series. This paper built the YOLO-SOD-DLKA architecture by introducing D-LKA module and an additional detection head for small and dense objects into YOLOv8 framework to detect astrocytes and nucleus.

The YOLOv8 framework has made multiple improvements based on previous versions such as C2f module, Decoupled Head and DFL Loss+IOU Loss classification loss function, which improves recognition accuracy and flexibility for various images and objects. We choose YOLOv8 as base framework and upgraded it with ability of adjusting attention area dynamically of D-LKA module. YOLO-SOD-DLKA model outperformed YOLOv8 on mAP@0.5 by 0.25%. It's reasonable to infer that our proposed architectures achieved desired performance in object detection and classification of astrocytes immunofluorescence photographs.

6. Conclusion

This paper proposed a method based on deep learning to analyze and quantify the positive expression of inflammatory factors in astrocytes immunofluorescence staining photographs automatically, efficiently and accurately. Our YOLO-SOD-DLKA model achieved 91.85% on mAP@0.5 in astrocytes and nucleus detection. The accuracy of the two proposed models met the requirement of quantify the level of positive expression of inflammatory factors. The architectures in this paper provided the practical method to analyze

other kinds of fluorescent photographs by artificial intelligence technology.

References

[1] C.J. Henry et al., “Peripheral lipopolysaccharide (LPS) challenge promotes microglial hyperactivity in aged mice that is associated with exaggerated induction of both pro-inflammatory IL-1beta and anti-inflammatory IL-10 cytokines,” Brain Behav Immun, vol. 23, no. 3, pp. 309-317, Mar. 2009, 10.1016/j.bbi.2008.09.002.

[2] P. Hasel et al., “Neuroinflammatory astrocyte subtypes in the mouse brain,” Nat Neurosci, vol. 24, no. 10, pp. 1475-1487, Oct. 2021, 10.1038/s41593-021-00905-6.

[3] R. Girshick et al., “Rich Feature Hierarchies for Accurate Object Detection and Semantic Segmentation,” in Proc. CVPR, Columbus, OH, USA, 2014, pp. 580-587.

[4] S. Ren et al., “Faster R-CNN: Towards Real-Time Object Detection with Region Proposal Networks,” IEEE Trans. Pattern Anal., vol. 39, no. 6, pp. 1137-1149, Jun. 2017, 10.1109/TPAMI.2016.2577031.

[5] J. Redmon et al., “You Only Look Once: Unified, Real-Time Object Detection,” in Proc. CVPR, Las Vegas, NV, USA, 2016, pp. 770-788.

[6] J. Redmon and A. Farhadi, “YOLO9000: Better, Faster, Stronger,” in Proc. CVPR, Honolulu, HI, USA, 2017, pp. 6517-6525.

[7] J. Redmon and A. Farhadi, “YOLOv3: An Incremental Improvement,” ArXiv e-prints, 2018, 10.48550/arXiv. 1804.02767.

[8] A. Bochkovskiy, C. Wang and H.M. Liao, “YOLOv4: Optimal Speed and Accuracy of Object Detection,” ArXiv e-prints, 2020, 10.48550/arXiv.2004.10934

[9] Y. Zhou and P. Fei, “China's Top 10 Optical Breakthroughs: Deep Learning-Enhanced High-Throughput Fluorescence Microscopy.” Laser&Optoelectronics Progress, vol. 61, no. 14, pp. 1400001-1-1400001-8, Jul. 2024, 10.3788/LOP232549.

[10] R. Azad et al., “Beyond Self-Attention: Deformable Large Kernel Attention for Medical Image Segmentation” in Proc. WACV, Waikoloa, HI, USA, 2024; pp. 1276-1286.

[11] C. Lam et al., “Automatic detection of diabetic retinopathy using deep learning based on retinal image,” AMIA Jt Summits Transl Sci Proc. 2018, pp. 147-155.

[12] S. Zheng et al., “Automatic Pulmonary Nodule Detection in CT scans Using Convolutional Neural Networks Based on Maximum Intensity Projection,” IEEE Transactions on Medical Imaging, vol. 39, no.3, pp. 797-805, Mar. 2020.

[13] L. Xue et al., “A real-time multi-class detection method for colonoscopypolyps based on improved YOLOv5s,” Journal of Hebei University (Natural Science Edition), vol. 44, no. 4, pp. 424-432, Apr. 2024.

[14] J. Sobek et al., “MedYOLO: A Medical Image Object Detection Framework,” ArXiv e-prints, 2023, arXiv:2312.07729.